EPSC Abstracts
Vol. 13, EPSC-DPS2019-1167-3, 2019
EPSC-DPS Joint Meeting 2019

EPSC
EPSC-DPS Joint Meeting 2019
15–20 September 2019 | Geneva, Switzerland

Cassini VIMS observations of Saturn's rings on the Grand Finale orbits

Philip D. Nicholson (1), Matthew M. Hedman (2), Stéphane Le Mouélic (3), Gianrico Filacchione (4) and Roger N. Clark (5).
(1) Department of Astronomy, Cornell University, Ithaca NY 14853, USA (2) Department of Physics, University of Idaho, Moscow ID 83844, USA (3) Laboratoire de Planetologie et Geodynamique, CNRS-UMR 6112, Université de Nantes, 44322 Nantes, France (4) IAPS-INAF, via Fosso del Cavaliere, 100, 00133 Rome, Italy (5) Planetary Science Institute, 1700 East Lowell, Suite 106, Tucson AZ 85719 (nicholso@astro.cornell.edu).

1. Introduction

The reflectance spectrum of Saturn's rings in the UV, visible and near-IR regions is dominated by fine-grained crystalline water ice with relatively small amounts of non-icy material [14, 16, 8, 3]. The latter is generally thought to be either organic in nature or nano-phase particles of metallic iron or iron-oxides, combined with silicates and/or carbon deposited by interplanetary debris [9, 6, 17, 7, 4, 1]. This icy mixture makes up the regolith coating the surfaces of the individual millimeter- to meter-sized ring particles.

2. Observations

Previous observations by the VIMS instrument on Cassini have revealed significant regional-scale spatial variations in the rings' visible and near-IR spectrum [15, 10, 11, 13]. The final, or 'Grand Finale' orbits of the Cassini mission provided an opportunity for spectral scans across the entire ring system at a spatial resolution unmatched since the more limited observations at Saturn Orbit Insertion (SOI) in 2004, covering both the sunlit and unlit sides of the rings. For each spectral scan, the instrument stared in a fixed inertial direction while the motion of the spacecraft carried the field of view across the rings at a radial velocity of 7–9 km/s, resulting in a single, continuous image 64 pixels wide by ~ 1000 pixels long with a spatial resolution of 30–60 km. On revs 255 and 262, the aim point moved outwards across the sunlit rings, so that the resolution is highest in the A ring. On rev 287, on the other hand, the aim point moved inwards, resulting in the resolution being highest in the C ring. The unlit side of the rings was scanned on revs 260 and 262. The phase angle was $\sim 65^\circ$ for the lit side scans and $\sim 130^\circ$ on the unlit side.

3. Results

Overall, the main features seen in the spectral profiles are very similar to those seen in the VIMS spectra acquired at SOI [15] and in previous spectral scans of the sunlit rings [10, 13]. At regional scales, we see that the ice band depths are greatest in the outer half of the B ring and the outer two-thirds of the A ring, and lowest in the inner C ring and the Cassini Division. As noted in previous studies, there are no abrupt transitions between the major ring regions. Instead, the band depths decrease smoothly from the middle A ring into the outer Cassini Division, and also from the innermost part of the B ring into the outer C ring, and then decrease further across the C ring. Our initial results were summarized by [18]. We focus here on the B ring.

Figure 1 shows the standard VIMS spectral parameters for the B ring, derived from the VIMS lit-side scan on rev 287, at a sampling interval of 20 km. Plotted here are water-ice band depths calculated from the average spectrum of each radial bin, using the formula [2]:

$$D_B = 1 - \frac{S(\lambda_0)}{S(\mathrm{ref})} \tag{1}$$

where $S(\lambda_0)$ is the I/F at the bottom of the band and $S(\mathrm{ref})$ is an average of the I/Fs at reference wavelengths on either side of the band. Also shown are the normalized spectral slopes in the visible portion of the spectrum, between 0.35 and 0.55 μm and between 0.55 and 0.85 μm. For further details, see [15] and [10]. Previous observations have shown that the UV slope is strongly correlated with the IR ice band depths, with both increasing as either the ice grain size in the particle regolith increases or the abundance of non-icy material decreases.

In the B ring, we again find that the UV slope is strongly correlated with the IR ice band depths, most notably in the complex region between radii of 99,000 and 104,000 km, referred to as B2 by [5]. This region is characterized by a series of abrupt local transitions in optical depth $\tau_{\rm n}$, between ~ 2 and 5 or more, at irregular intervals of $50 - 200$ km. Close inspection of the VIMS data shows that there is an almost-perfect positive correlation between the ice band depths, the UV slope and $\tau_{\rm n}$, with every peak (or dip) in band depth being associated with a maximum (or minimum) in $\tau_{\rm n}$, as first reported by [13]. Interestingly, the correlation of band depths with I/F is much weaker, with peaks in band depth being associated with both maxima and minima in I/F in this region. Outside the B2 region, we find that there are only minimal variations in band depth or UV slope across the B ring, except for the outermost ~ 1300 km or so.

Measurements of the precise wavelength of the broad continuum peak at $\sim$ 3.6 μm can be used to infer the surface temperature of the ring particles [12], and its spatial and temporal variations. Across the B ring, the regolith temperature inferred in this manner shifts from $T = 88$ K at radii greater than 105,000 km to 107 K in the inner B ring, indicating that the particle surfaces are colder where the optical depth and reflectivity are higher.

Acknowledgements

We acknowledge generous support from the Cassini Project, via NASA, ESA, ASI and CNRS. The work presented here was made possible by the contributions of many other members of the VIMS science and engineering teams in the US, Italy, France, the UK and Germany.

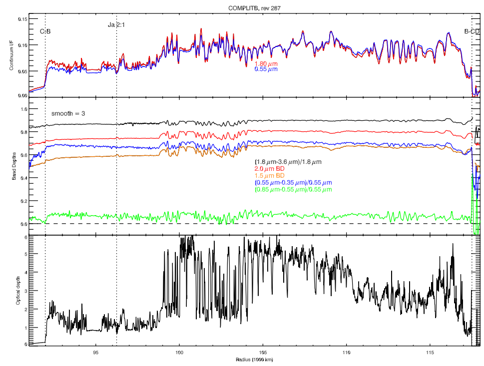

Figure 1: Radial profiles of IR spectral parameters for the B ring derived from the VIMS lit-side scan on rev 287, rebinned to a uniform sampling resolution of 20 km. The upper panel shows the reflectivity of the rings at continuum wavelengths of 0.55 and 1.8 μm. The middle panel shows the fractional depths of the water ice bands at 1.55, 2.0 and 3.6 μm, coded by line color, as well as the visible spectral slopes (see text for definitions), all smoothed to a resolution of 60 km. The lower panel shows an optical depth profile of the rings obtained from a VIMS stellar occultation on rev 82, binned to 10 km resolution, as context.

References

[1] Ciarniello, M. *et al.*, 2019. Icarus 317, 242-265.

[2] Clark, R. N., Roush, T. L. 1984. Journal of Geophysical Research 89, 6329-6340.

[3] Clark, R. N., Fanale, F. P., Gaffey, M. J. 1986. In "Satellites", U. Arizona Press, 437-491.

[4] Clark, R. N., *et al.*, 2012. Icarus 218, 831-860.

[5] Colwell, J. E., *et al.*, 2009. In "Saturn from Cassini-Huygens", Springer, 375-412.

[6] Cuzzi, J. N., Estrada, P. R. 1998. Icarus 132, 1-35.

[7] Cuzzi, J., *et al.*, 2009. In "Saturn from Cassini-Huygens", Springer, 459-509.

[8] Esposito, L. W., *et al.*, 1984. In "Saturn", U. Arizona Press, 463-545.

[9] Estrada, P. R., Cuzzi, J. N. 1996. Icarus 122, 251-272.

[10] Filacchione, G., *et al.*, 2012. Icarus 220, 1064-1096.

[11] Filacchione, G., *et al.*, 2013. The Astrophysical Journal 766, 76.

[12] Filacchione, G., *et al.*, 2014. Icarus 241, 45-65.

[13] Hedman, M. M., *et al.*, 2013. Icarus 223, 105-130.

[14] Lebofsky, L. A., Johnson, T. V., McCord, T. B. 1970. Icarus 13, 226-230.

[15] Nicholson, P. D., *et al.*, 2008. Icarus 193, 182-212.

[16] Pilcher, C. B., *et al.*, 1970. Science 167, 1372-1373.

[17] Poulet, F., *et al.*, 2003. Astronomy and Astrophysics 412, 305-316.

[18] Tiscareno, M. S., *et al.*, 2019. Science (in press).